The behavior of a compressible silty fine sand

An-Bin Huang, Huai-Houh Hsu, and Jia-Wei Chang

Abstract: Publications associated with sands are often limited to clean (i.e., little fines content), uniform, uncemented silica or quartz sand. On the other hand, the importance of mineral content, particle shapes, as well as gradation to the behavior of sand has long been recognized. Although systematic studies of sands other than clean quartz sand have been limited, there is increasing attention being paid to sands with an appreciable fines content. Because of a major construction project, extensive field and laboratory experiments were performed on a silty fine sand from Mai-Liao, which is located on the central west coast of Taiwan. Results show that Mai-Liao Sand (MLS), a silty sand, can be significantly more compressible than clean quartz sand under static load. The particles of MLS have moderate strength, and significant crushing can be induced by triaxial shearing. As a result, MLS has low dilatancy and a relatively small range of peak friction angles. Cone penetration tests in MLS were conducted in a calibration chamber. Analyses of the data indicate that interpreting cone tip resistance in MLS using methods developed based on clean quartz sand without considering the differences of compressibility can be unrealistic. This paper documents results of the experimental studies on MLS.

Key words: silty fine sand, strength, dilatancy, compressibility, crushing, in situ test.

Résumé : Les publications associées aux sables se limitent souvent aux sables quartziques ou siliceux propres (peu de fines), uniformes et non cimentés. Par ailleurs on a reconnu depuis longtemps que le comportement de ces matériaux était fortement tributaire de la partie minérale, de la forme des particules ainsi que de la répartition granulométrique. Bien qu'il n'existe qu'un petit nombre d'études systématiques sur les sables autres que les sables quartziques propres, ceux qui contiennent un part appréciable de fines retiennent de plus en plus l'attention. A l'occasion d'un important projet de construction, on a effectué des essais complets, en place et au laboratoire, sur un sable fin silteux de Mai-Liao, sur la côte centre-ouest de Taiwan. Les résultats indiquent que le sable de Mai-Liao (MLS) peut être beaucoup plus compressible, sous charge statique, qu'un sable quartzique propre. Les particules de MLS ont une résistance modérée et un cisaillement triaxial peut provoquer un broyage significatif des grains. Ainsi le MLS présente-t-il une dilatance faible et un intervalle relativement étroit d'angles de frottement au pic. Des essais de pénétration au cône ont été effectués sur le MLS dans une chambre de calibration. L'analyse des données indique qu'il peut être irréaliste d'interpréter la résistance de pointe selon des méthodes développées pour des sables propres, sans considérer les différences de compressibilité. Cet article présente les résultats des essais expérimentaux sur le MLS.

Mots clés : sable fin silteux, résistance, dilatance, compressibilité, broyage, essai in situ.

[Traduit par la Rédaction]

Introduction

Publications associated with sands are often limited to clean (i.e., little fines content), uniform, uncemented silica or quartz sand. The sands generally have a low compressibility under normal, static loading conditions. The relationships among confining stress, void ratio, strength, and dilatancy are expected to follow a certain pattern. There are empirical rules or analytical models developed either for test result interpretation or for design of foundations for such sand. On the other hand, the importance of mineral content, particle shapes, as well as gradation to the behavior of sand has long been recognized (Koerner 1970*a*, 1970*b*; Joustra and de Gijt 1982; Ishihara 1993). Although systematic studies of sands other than clean quartz sand have been limited, increasing attention is being paid to sands with an appreciable amount of fines. The silty fine sand referred to in this paper can have significant amounts of fines; it constitutes most of the natural sand deposits along the west coast of Taiwan. The sand deposit has depths typically in the range of several hundred metres.

This paper compiles available data on the silty fine sand from a test site in Mai-Liao, which is located on the central west coast of Taiwan. Extensive soil borings and in situ tests have been performed on Mai-Liao Sand (MLS) for various purposes related to the project. In addition to data collected for engineering purposes, a series of research-quality laboratory experiments have been performed to establish a comprehensive database. Chamber calibration tests of cone penetration tests (CPT) were performed to establish an interpretation method for CPT in MLS. The data were analyzed and organized using some of the existing frameworks to describe the characteristics of this silty sand and to propose a method for determining geotechnical engineering parameters using CPT.

Received November 7, 1997. Accepted October 7, 1998.

A.-B. Huang, H.-H. Hsu, and J.-W. Chang. Department of Civil Engineering, National Chiao-Tung University, Hsin-Chu, Taiwan.

Test site

This paper concentrates on data collected at a test site where a total of 50 borings were conducted. Figure 1 shows

Fig. 1. General layout of the Mai-Liao project site and soil boring locations.

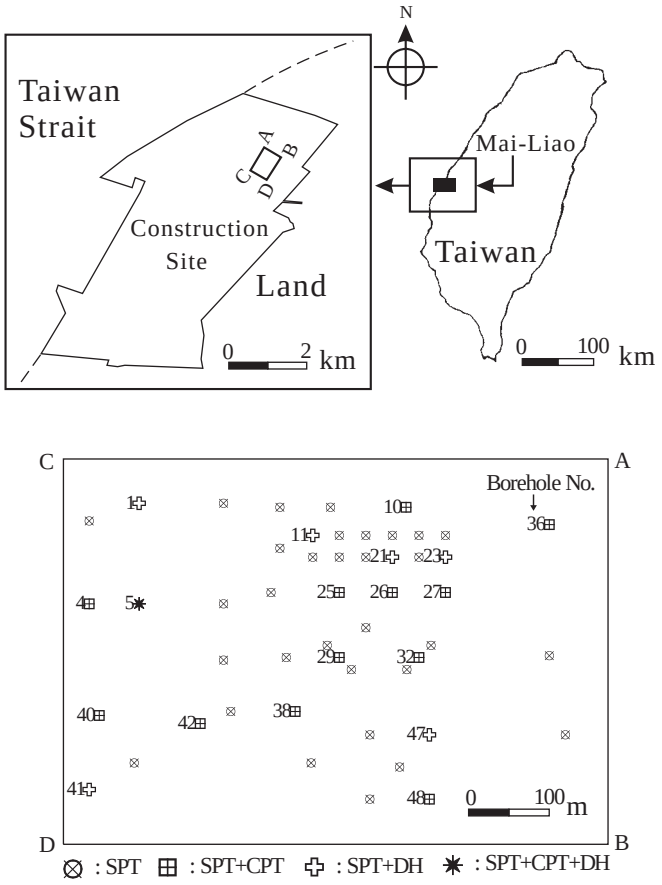

the general location and dimensions of the test site (marked ABCD) and its relationship with a petrochemical construction project area. Reclaimed land in excess of 2400 ha that extends the original shoreline further into the ocean is under construction in this area. The original ground surface was at a maximum of 2–3 m below sea level. Major construction activities included dredging sand offshore and transporting and placing it onshore as a hydraulic fill. The placement of the hydraulic fill would raise the grade to approximately 3 m above sea level. The hydraulic fill along with its underlying natural deposits are subsequently densified using dynamic compaction. The in situ tests in this area included standard penetration tests (SPT), CPT, and down-hole (DH) seismic shear wave velocity measurements. Locations of these boreholes are shown in Fig. 1. The borehole number is shown in Fig. 1 only when data retrieved there are utilized later in the paper.

Geological origin and physical properties of MLS

MLS came from the central mountain range that lies longitudinally on the east side of Taiwan. Sedimentary and metamorphic rocks were deteriorated and flushed by rainfalls through steep slopes and rapidly flowing streams before settling down on the west plain. The process of transportation ground the fractured rock into sand and silt particles. Figure 2 compiles the blow counts per 30 cm of penetration, N from SPT, cone tip resistance, q_c, from CPT, and fines (particles pass No. 200 sieve) content profiles from 13 of the borings shown in Fig. 1. The shear wave velocities shown in Fig. 2 were collected from seven test locations. The fines of MLS are mostly nonplastic; the in situ fines contents varied from less than 10 to over 90%. The soil deposit is generally classified as SM or ML, depending on the amount of fines content. The ML material is mostly found below a depth of 10 m.

A batch of 20 tons of MLS was taken from within a depth of 2 m at the test site to provide specimens for laboratory consolidation, triaxial, and CPT calibration chamber tests. The sand was sieved to filter out leaves or gravel-sized particles and then kiln-dried. The drying process also serves to mix and unify the gradation of sand taken from the field. MLS has a dark gray color. Figure 3 shows grain size distribution curves from four randomly selected specimens of the kiln-dried MLS. Apparently, the drying and mixing process has effectively unified the sand gradation. Essentially all particles pass a No. 60 sieve; the fines contents of the four kiln-dried specimens have an average value of 15.1%. For comparison purposes, grain size distribution curves from field samples obtained in various boreholes are also included in Fig. 3 (broken curves). The 15% fines content is more representative for MLS within top 10 m in the field. The kiln-dried MLS has a maximum dry unit weight ($\gamma_{d\ max}$) of 16.6 kN/m^3 and a minimum dry unit weight ($\gamma_{d\ min}$) of 12.8 kN/m^3. The specific gravity of MLS has an average value of 2.69. X-ray diffraction analysis on MLS showed significant contents of muscovite and chlorite in addition to quartz. The grain shapes of particles retained on a No. 200 sieve are subangular to angular and flaky, as indicated by the scanning electronic micrographs shown in Fig. 4.

Field characterization of MLS

According to the SPT and CPT profiles shown in Fig. 2, the soil conditions throughout the test site are fairly uniform in the lateral direction. For a given depth, the q_c and N values are confined to a relatively narrow range. The q_c, maximum shear modulus, G_{max}, from DH shear wave velocity measurements, and N values from SPT were collected at comparable depths from various boreholes to facilitate comparisons with previously reported relationships. The ratios of q_c, normalized with respect to atmospheric pressure P_a, over N as shown in Fig. 5 are erratic but indicate a trend of a slightly negative relationship between q_c/P_aN and fines content, as suggested by Kulhawy and Mayne (1991). The field SPT was conducted with various types of hammers, without energy calibration. A significant part of that erratic correlation may be due to the variations of test equipment and (or) energy efficiency involved in the available SPT data. For MLS and the available data, the correlation between N and q_c is not strong enough to justify the application of the empirical equation suggested by Kulhawy and Mayne (1991).

Figure 6 shows a correlation between G_{max} and q_c for the MLS and that proposed by Rix and Stokoe (1991) for quartz sands. The majority of the MLS data points fall below the Rix and Stokoe correlation, indicating a lower stiffness (lower G_{max} for the same q_c), lower peak strength of MLS (lower q_c for the same vertical stress σ_v'), or both.

Fig. 2. Profiles of in situ tests.

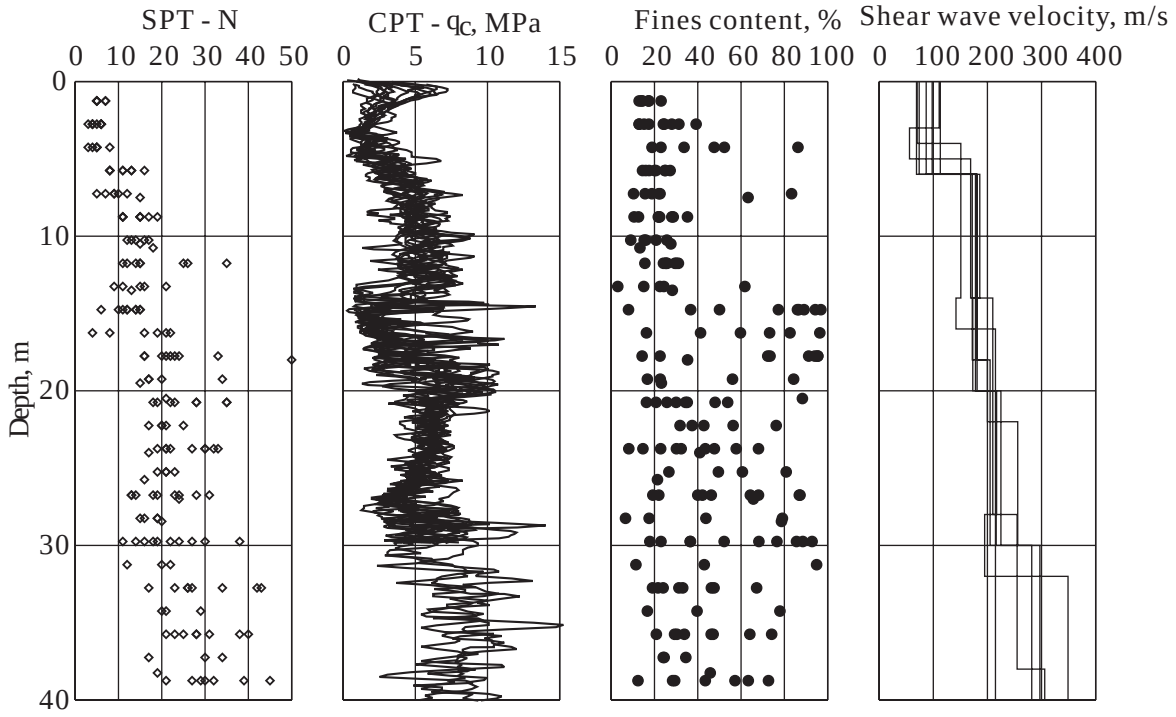

Compressibility of MLS

Compressibility of sand under static conditions is usually low, at least for quartz sand, except when the stress is extremely high. Under high-stress conditions, the compression of sand is mainly a result of particle crushing. Extensive studies on compression and crushing of granular materials under elevated stresses have been reported (Lee and Farhoomand 1967; Vesic and Clough 1968; El-Sohby and Andrawes 1972; Hardin 1985; Been et al. 1991; Lade et al. 1996; Yamamuro et al. 1996; Konrad 1998). The compressibility of MLS was measured isotropically in a triaxial cell and one-dimensionally in an oedometer using the kiln-dried material.

The isotropic consolidation tests were performed on specimens, 70 mm in diameter and 150 mm high, prepared in membrane-lined split mould mounted on the lower platen of the triaxial cell. Dry sand was first placed in the mould using a spoon and then statically pressed to achieve the desired void ratio in four equal layers. Because of the high compressibility of MLS, to be described later, static pressing was rather effective in densifying the sand specimen without causing particle segregation. To verify the uniformity of gradation, a specimen was prepared following this procedure and then saturated in the triaxial cell under an effective confining stress of 30 kPa. The confining stress was then released and the specimen removed from the triaxial cell. The specimen was sliced into nine equal layers. Table 1 shows the fines content measured for each of the nine layers. They varied from 14.6 to 16.2% with an average of 15.3%, which is 0.2% higher than the average of those shown in Fig. 3. No sign of concentration of fines was noticed.

The specimen was saturated under a back-pressure of 98.1 kPa prior to the doubly drained isotropic consolidation test in the triaxial cell. A burette was connected to the drainage lines of the triaxial specimen. The water level in the burette was monitored by a differential pressure transducer. The amount of porewater drainage in and out of the specimen during the isotropic consolidation was monitored by measuring the porewater level fluctuation in the burette. Figure 7 shows a set of isotropic consolidation curves in terms of void ratio versus effective mean normal stress (e – log p'). The maximum void ratio (e_{max} = 1.04) and the minimum void ratio (e_{min} = 0.57) of MLS are indicated in Fig. 7 to provide a reference of relative density, D_r, for the consolidation curves. The step-loading consolidation tests had a maximum consolidation stress of 588 kPa.

The primary compression index taken as the slope of the e – log p' curve near the maximum consolidation stress is approximately 0.08 ± 0.01. The swelling index or slope of the rebound part of the e – log p' curve is 0.013 ± 0.002. These compression indices are unusually high for a sand under such mild stress conditions. The consolidation stress was maintained for 60 min for each load increment to facilitate observations of secondary consolidation. The time settlement record provided a set of void ratio – time (e – log t) curves to determine the secondary compression index. The ratios of primary over the secondary compression indices (equivalent to C_α/C_c in one-dimensional compression) taken beyond the apparent preconsolidation stress varied from 0.02 to 0.025, which is within the range of sand and sandy silt in one-dimensional compression, as reported by Mesri et al. (1990). The whole specimen was used for a sieve analysis after the consolidation test. The change in fines contents was within 1% compared with the average fines content of 15.1% shown in Fig. 3. The difference is likely to be within the accuracy of the experiments, indicating that the volume change was mainly a result of rearrangement of sand parti-

Fig. 3. Grain size distribution of MLS.

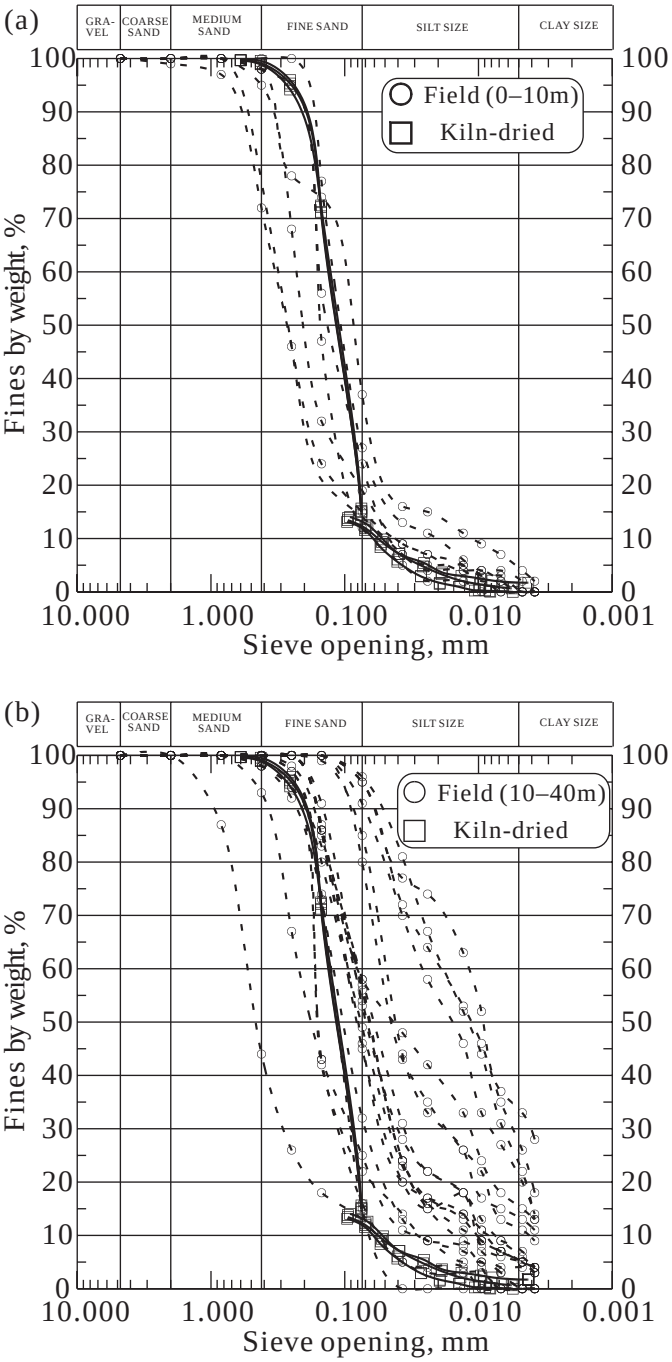

Fig. 4. Scanning electronic micrographs of MLS. (*a*) Particles retained on a No. 200 sieve; (*b*) particles passing a No. 200 sieve.

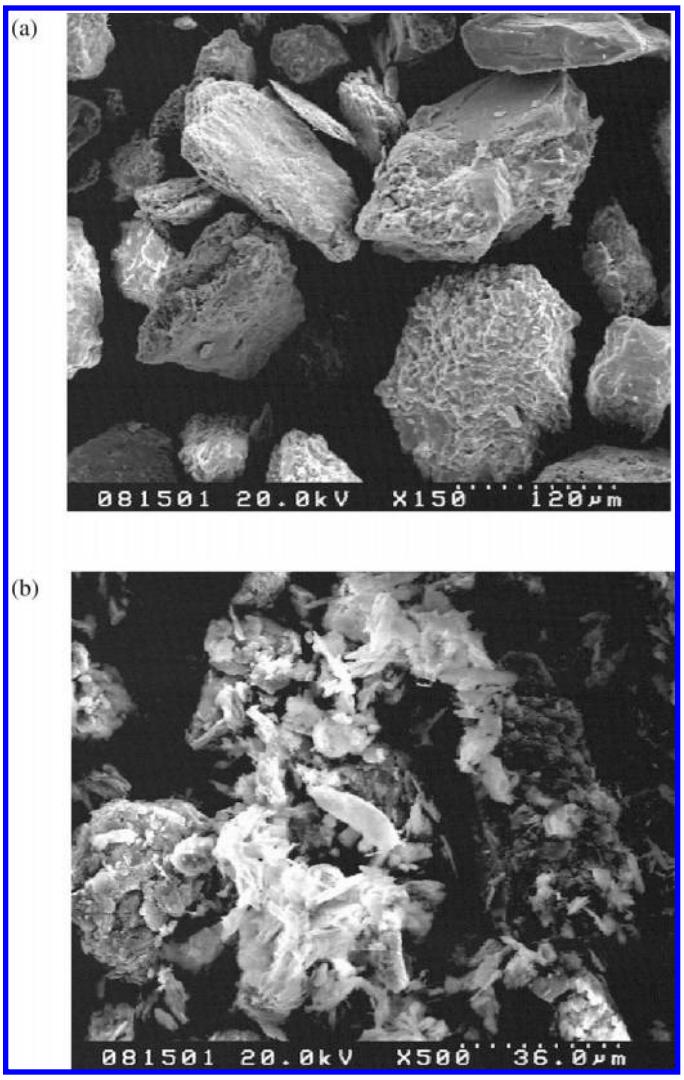

cles and crushing was minimal.

In order to facilitate further comparisons with quartz sand in compressibility and crushing, one-dimensional consolidation tests under elevated stress conditions were conducted on MLS. A high-capacity, strain-controlled load frame originally designed for creep tests on rock specimens was used for the consolidation tests. The sand specimen was prepared in a thick, oil-impregnated bronze ring 70 mm in diameter and 25 mm high. The specimen was inundated in water as in the case of a step-loading consolidation test. The vertical deformation of the specimen was monitored using a linear displacement transducer and the vertical stress measured with a load cell. A strain rate of 0.065%/min was used in these tests. This strain rate is approximately 10 times that of the isotropic step-loading consolidation tests described above. Figure 8 shows e versus vertical consolidation stress, σ_v', from the one-dimensional consolidation tests with three different initial void ratios. The specimens were consolidated to a maximum consolidation stress of 10 MPa. A comparison with quartz sand (see Fig. 8) under similar loading conditions shows that MLS is at least five times as compressible as quartz sand, depending on the stress level and density. Results show a further increase of compressibility beyond the maximum stress level applied in the isotropic consolidation (i.e., 588 kPa). The one-dimensional compression index according to the e – log σ_v' curves at σ_v' values between 3 and 10 MPa, where three curves essentially

Fig. 5. Variation of q_c/P_aN with fines content.

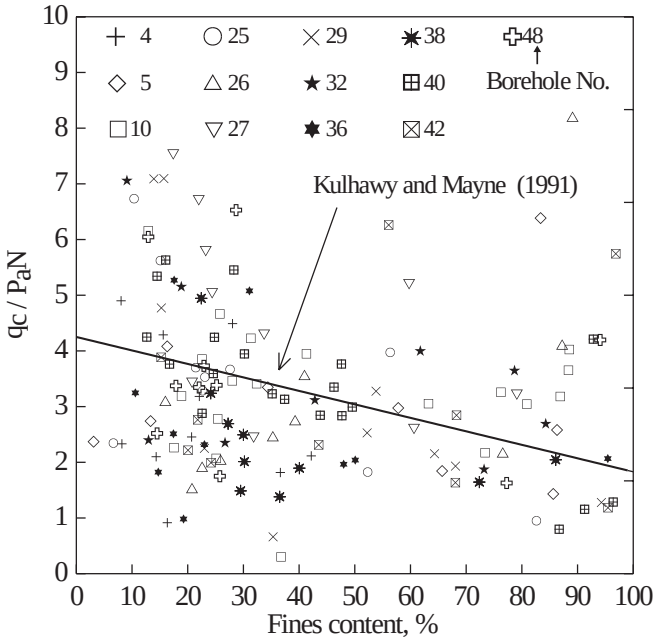

Fig. 6. Correlation between G_{max} and q_c of MLS.

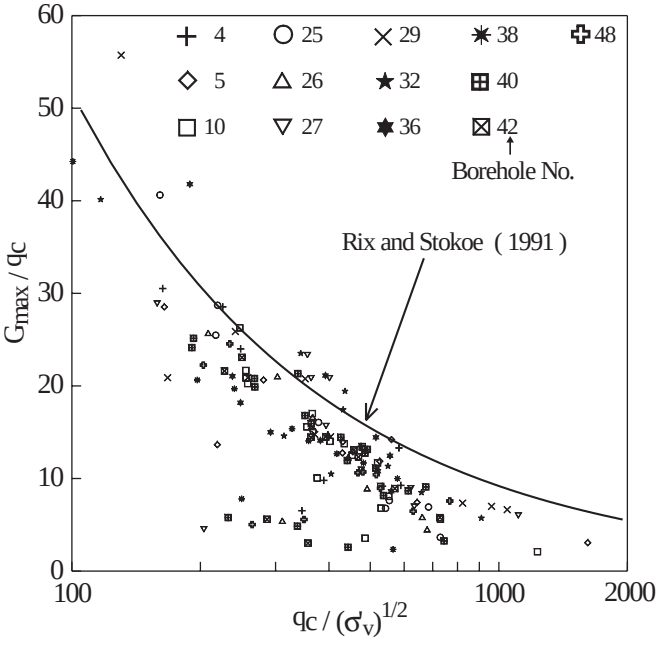

Table 1. Vertical distributions of fines content of the triaxial specimen.

Layer No.	Height (mm)	Fines content (%)
1	0–17	15.3
2	17–34	15.7
3	34–51	16.2
4	51–68	15.4
5	68–86	14.6
6	86–103	14.7
7	103–120	15.3
8	120–137	15.4
9	137–154	15.4

Fig. 7. e – log p' curves from isotropic consolidation tests.

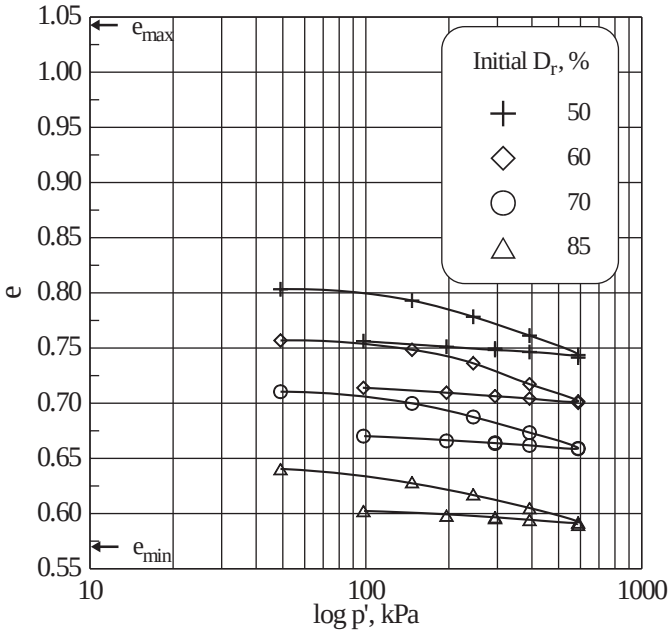

Fig. 8. e – log σ_v' curves from one-dimensional consolidation tests.

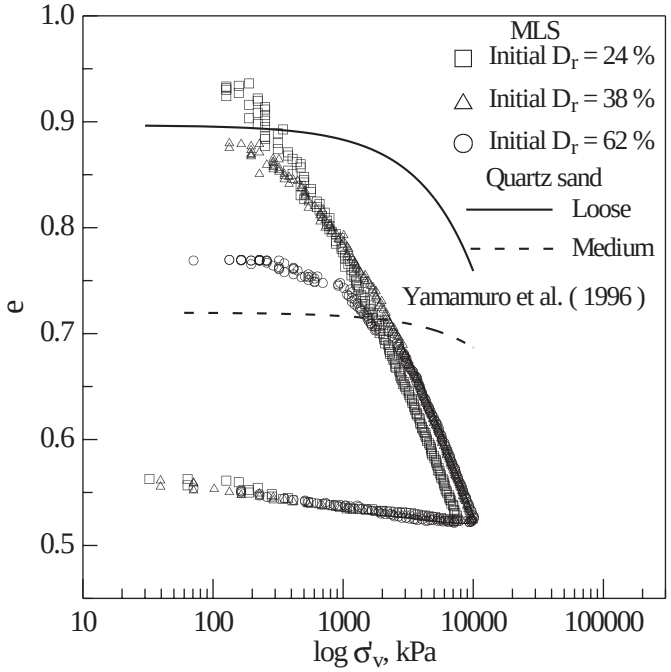

merge together, is approximately 0.29. This compression index value is comparable with that of a lean clay. The whole specimen was used in the measurement of fines content following the consolidation test. All three specimens showed an increase of fines content of approximately 3% after the test. Judging from the moderate increase of fines content, it appears that the compression of MLS under one-dimensional loading is again mostly a result of rearrangement of soil particles.

Hardin (1985) indicated that most crushing occurs to particles with diameters larger than silt size ($D \geq 0.074$ mm).

Table 2. Variables applied in the MLS triaxial tests.

Initial void ratio, e_0	Initial D_r (%)	Effective confining stress, σ_c' (kPa)				
0.80	50	49.0	147.1	245.2	392.3	588.4
0.76	60	49.0	147.1	245.2	392.3	588.4
0.71	70	49.0	147.1	245.2	392.3	588.4
0.64	85	49.0	147.1	245.2	392.3	588.4

Following this concept, a breakage potential B_p can be computed as the area between the line defining the upper limit of silt size, D = 0.074 mm, and the part of the particle size distribution curve for which D > 0.074 mm. According to Hardin's (1985) definition and the grain size distribution curves shown in Fig. 3, the MLS has a B_p of approximately 0.21. This B_p is less than the lowest value reported by Hardin (1985) for various sands. The low B_p values are consistent with the small amounts of crushing observed in consolidation tests.

Shear strength, dilatancy, and crushing of MLS

A series of isotropically consolidated drained (CID) triaxial tests with volume change measurements were performed on the kiln-dried MLS. The main objective of these tests is to evaluate the strength and dilatancy characteristics of MLS. A total of 20 CID triaxial tests were performed with combinations of four levels of initial relative densities and five levels of effective confining stress. Variables applied in this series of triaxial tests are summarized in Table 2.

The triaxial specimens were prepared following the same procedure as previously described for isotropic consolidation tests. Upon preparation, the triaxial specimen was flushed with carbon dioxide and then deaired water. A back-pressure of 98.1 kPa was used in all tests to assure saturation and the specimens had a minimum B value of 0.97. The variation of void ratio during specimen consolidation was measured following the same procedure as used in isotropic consolidation tests. The change of void ratio resulting from consolidation was deducted in the analysis. Triaxial shearing was applied through strain-controlled axial compression at a rate of 0.1%/min. No lubrication was applied to the end platens, as the specimen height over diameter ratio exceeded 2; consequently, the effect of end friction was expected to be minimal (Bishop and Green 1965). Because of the fine nature of the sand particles, membrane penetration was not expected to be significant. Figure 9 shows a set of the CID triaxial tests on specimens with initial D_r of 50%. The data are presented in terms of deviator stress ($\sigma_1' - \sigma_3'$) and volumetric strain (ε_v) versus axial strain (ε_a).

The concepts of relative dilatancy index, I_R (Bolton 1986), and state (Been and Jefferies 1985) are used to evaluate the triaxial test data as they relate to strength and dilatancy. Bolton (1986) suggested that the drained peak friction angle, ϕ'_{max}, should be obtained by dropping a tangent from the origin to a single Mohr circle (i.e., a secant friction angle) that represents the maximum deviator stress conditions from a triaxial test. The secant drained friction angle under the critical state (i.e., a condition where shearing continues without volume change), ϕ'_{crit}, is mainly a function of mineral content of the sand. The ϕ'_{crit} of MLS measured from triaxial tests on loose specimens under critical state varied from 30.8 to 32.4° with an average value of 31.6°. The ϕ'_{crit} is comparable with the lower end of a quartz sand. This is apparently due to the contents of softer minerals such as muscovite and chlorite.

Fig. 9. CID triaxial test results with an initial D_r of 50%.

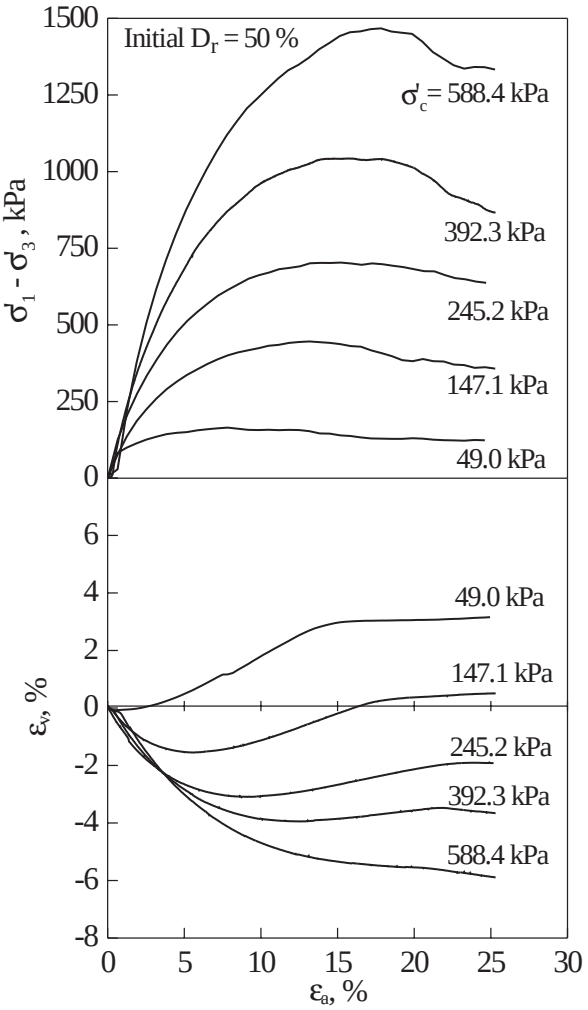

Figure 10 shows a plot of $\phi'_{max} - \phi'_{crit}$ versus p'_p from triaxial tests on MLS in which p'_p is the mean effective stress at peak deviator stress. According to Bolton (1986), I_R combines the effects of sand density and confining stress; empirically:

$$[1] \qquad I_R = \frac{D_r}{100}\left(Q - \ln\left(\frac{100 p'_p}{P_a}\right)\right) - 1$$

where Q is an empirical constant that increases with the crushing strength of sand grains and P_a is the atmospheric pressure. For quartz or feldspar, Q = 10, and for chalk, Q = 5.5. I_R controls $\phi'_{max} - \phi'_{crit}$ and the maximum rate of dilation $(d\varepsilon_v/d\varepsilon_a)_{max}$ as

$$[2] \qquad \phi'_{max} - \phi'_{crit} = 3I_R^0$$

$$[3] \qquad \left(-\frac{d\varepsilon_v}{d\varepsilon_a}\right)_{max} = 0.3I_R$$

Fig. 10. $\phi'_{max} - \phi'_{crit}$ versus p'_p for MLS.

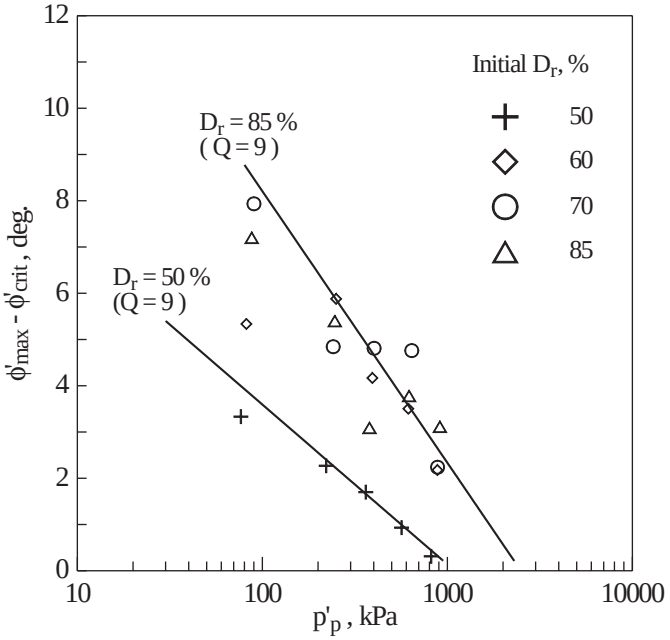

Fig. 11. Dilatancy of MLS during triaxial tests.

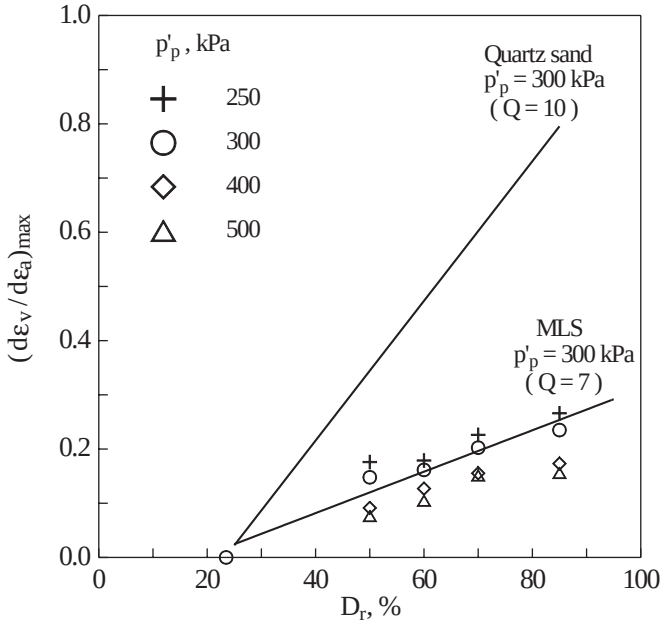

The range of $\phi'_{max} - \phi'_{crit}$ shown in Fig. 10 is at the lower end of similar values for quartz sands reported by Bolton (1986). The maximum rates of dilation $(d\varepsilon_v/d\varepsilon_a)_{max}$ of MLS in triaxial tests are significantly less than those for quartz sand reported by Bolton (1986) under comparable p'_p, as shown in Fig. 11. If eq. [2] is used to fit the available data points of MLS, Q should fall in the range between 7 and 9. The Q values correspond to those of limestone or anthracite according to Bolton (1986), indicating a mildly crushable nature of the MLS grains. No single Q value can provide a reasonable fit to the data points of $\phi'_{max} - \phi'_{crit}$ (Fig. 10) and $(d\varepsilon_v/d\varepsilon_a)_{max}$ (Fig. 11) simultaneously. Sieve analyses performed on MLS specimens within a thickness of 1 cm along the shear plane after the triaxial tests showed an increase in fines contents from 2 to 8% as p'_p varied from 50 to 800 kPa. The initial relative density of the triaxial specimen does not appear to have a significant effect on the increase of fines content induced by triaxial shearing. The low dilatancy and shearing-induced fines content increase indicate that $\phi'_{max} - \phi'_{crit}$ for MLS is likely a result of shearing and crushing of sand particles as well as dilation caused by particles overriding one another.

Figure 12 shows a comparison of critical state lines between MLS and Ticino sand, a clean, uniformly graded quartz sand. The combination of effective mean normal stress (p') and void ratio towards the end of triaxial tests shown in Fig. 9 (i.e., initial D_r of 50%) was used to establish the critical state line for MLS. The selection of critical state is approximate, as volume change continues in some of the triaxial tests, even at 25% of axial strain. The critical state line for Ticino sand is according to results reported by Konrad (1998). Been et al. (1991) have indicated that the critical state line is generally bilinear. Depending on the soil type, grain crushing occurs during shear when p' reaches 1–2 MPa according to earlier reports (Konrad 1998). The slope of the critical state line beyond crushing stress (λ_c) is much steeper due to changes in gradation and grain shape as a result of grain crushing. For MLS, the bilinear nature of the critical state line is not as clearly defined as for Ticino sand. The increase in fines after triaxial shearing, as described above, is an indication that crushing of sand grains or change of the slope of the critical state line occurs in MLS at a much lower stress.

Laboratory CPT calibration in the silty sand

There have been reports (McNeilan and Bugno 1984) indicating that cone penetration in silt or silty sand may not be a fully drained test. Due to positive excess pore pressure induced by the cone penetration, the cone tip resistance, q_c, in silty material may be lower as compared with tests in a clean sand with similar relative density. Dilatancy is another factor believed to have strong influence on q_c values (Yu and Houlsby 1991; Huang and Ma 1994; Salgado et al. 1997). The presence of fines and low dilatancy of MLS raised a question as to the validity of interpreting CPT using methods developed for clean, uniform quartz sand. A series of CPT chamber calibration tests were performed to address these issues.

Calibration chamber system and testing program

Figure 13 shows a schematic view of the calibration chamber. It was designed to house a 525 mm diameter and 760–815 mm high specimen. Chamber systems with similar dimensions have been reported (Bellotti and Pedroni 1991; Huang et al. 1991) and applied by others (Voyiadjis et al. 1993). The design makes a compromise between practicality in operation and the idea of having a large diameter ratio between chamber specimen and the cone. The relatively small chamber size was utilized for ease of saturation, backpressuring, and handling. The specimen diameter is 15 times that of a standard cone penetrometer (i.e., 35.6 mm). Apparently, CPT performed in a chamber with this diameter ratio will be subject to boundary effects (Parkin 1988) for clean

Fig. 12. Critical state lines and CPT initial states.

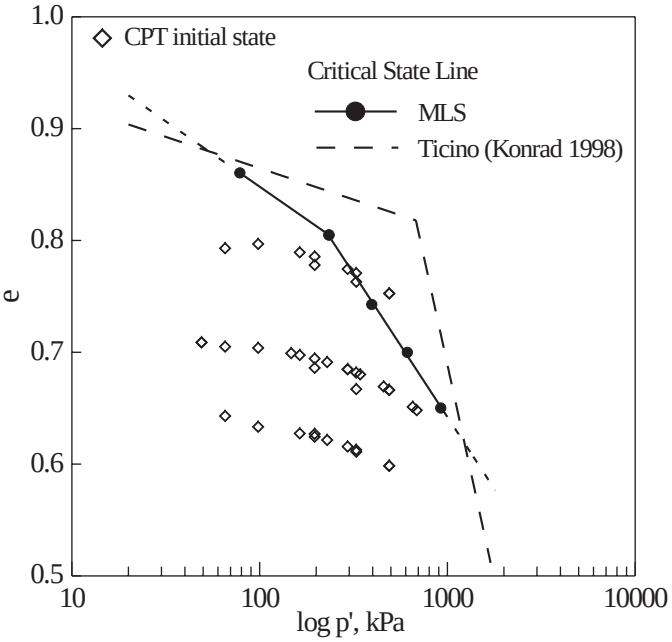

quartz sand. The chamber was designed to provide constant-stress lateral boundary conditions only.

The piston at the bottom of the specimen controls vertical stress. A sheet of 6.4 mm thick porous plastic is attached to the end plates to facilitate double drainage for the specimen. A total of six open-ended piezometers are installed on the bottom plate, as shown in Fig. 13. Two of the piezometers are located at a distance of dL = 25.4 mm from the center of the specimen, three at dL = 50.8 mm, and one at dL = 101.6 mm. The piezometers are made of 1.65 mm outside diameter, 0.23 mm wall stainless steel tubing filtered with a piece of nonwoven geotextile. The piezometer tips are at approximately 260 mm above the bottom of the specimen. Each piezometer is connected to a pressure transducer, as shown in Fig. 13. The voids within the piezometers and pressure transducer ports were filled with deaired glycerin. During saturation of the specimen, the piezocone is inserted in a sealed container at the top of the specimen. The container, made of delrin, also serves as a bushing.

Specimen preparation and testing procedure

The chamber specimen is prepared in a membrane-lined split mould, similar to the concept used in triaxial tests. The kiln-dried MLS was placed in a 500-kg bag initially, which in turn was lifted by a crane. A load cell was attached between the bag and the crane hook to monitor the weight of the bag. The specimen was created in four equal layers. The sand was slowly released from the bottom of the bag from immediately above the surface of deposition. This process minimizes the height of deposition, and thus the chance of segregation. The initial relative density upon deposition was approximately 50%. A 30 mm diameter and 500 mm long steel rod was inserted in the sand and rocked sideways to densify the sand. The locations of steel rod insertion were evenly distributed. Since the weight of each specimen layer was known, the density was monitored by the height of the specimen. The densification stopped when the desired specimen height was reached. This sand placement and densification process was repeated four times to create a specimen. Upon completion of sand deposition, a vacuum was applied to the sealed specimen and the membrane jacket removed. The vacuum was connected to the top of the piezocone container, the highest position of the chamber assemblage to be saturated. The chamber cell was then assembled and 30 kPa confining stress applied to the specimen.

Fig. 13. Schematic view of the calibration chamber.

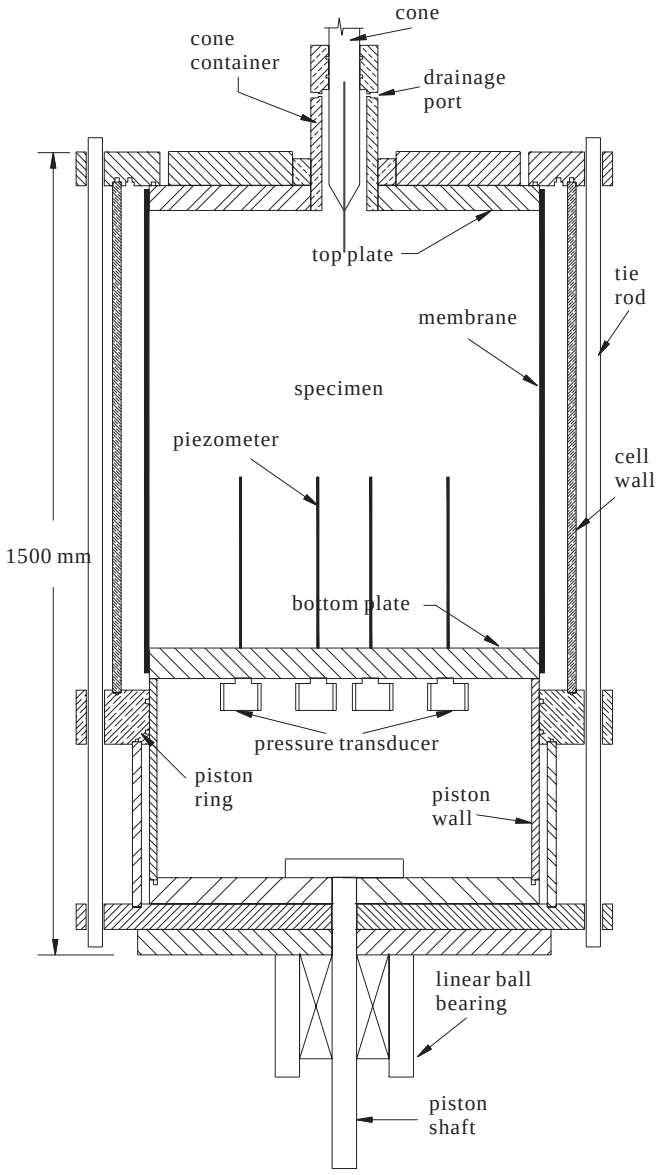

The piezocone tip was placed in a sealed container filled with glycerin and deaired under vacuum prior to installation in the chamber. The chamber and piezocone assemblage was bolted onto a hydraulic frame where cone penetration would take place.

The saturation process started by infiltrating CO_2 slowly from the bottom of the specimen under vacuum. The CO_2 circulation continued for approximately 30 min. Deaired water was then allowed to permeate from the bottom of specimen under vacuum. The permeation took approximately 3 h, until the piezocone container was flooded with water. A

Table 3. Variables applied in the calibration chamber tests and q_c results.

Test No.	Initial D_r (%)	Type of specimen	K	σ_v' (kPa)	p' (kPa)	Back-pressure (kPa)	q_c (MPa)
1	70	Saturated	1	49.0	49.0	98.1	5.99
2	70	Saturated	1	49.0	49.0	343.4	5.53
3	70	Saturated	1	98.1	98.1	98.1	8.41
4	70	Saturated	1	147.1	147.1	294.2	10.16
5	70	Saturated	1	196.1	196.1	294.2	11.50
6	70	Saturated	1	294.2	294.2	490.3	14.89
7	70	Dry	1	294.2	294.2	—	14.44
8	70	Dry	0.5	98.1	65.4	—	6.29
9	70	Dry	2	98.1	163.4	—	12.70
10	70	Dry	3	98.1	228.8	—	14.26
11	70	Dry	3	147.1	343.2	—	19.67
12	70	Dry	2	196.1	326.9	—	16.38
13	70	Dry	3	196.1	457.6	—	20.85
14	70	Dry	0.5	294.2	196.2	—	9.18
15	70	Dry	2	294.2	490.3	—	22.14
16	70	Dry	3	294.2	686.5	—	30.44
17	70	Dry	2	392.3	653.8	—	25.94
18	70	Dry	0.5	490.3	326.9	—	19.61
19	70	Dry	1	490.3	490.3	—	25.50
20	85	Dry	0.5	98.1	65.4	—	9.18
21	85	Dry	1	98.1	98.1	—	9.35
22	85	Dry	2	98.1	163.4	—	12.20
23	85	Dry	3	98.1	228.8	—	14.83
24	85	Dry	1	196.1	196.1	—	13.19
25	85	Dry	2	196.1	326.9	—	18.18
26	85	Dry	0.5	294.2	196.2	—	14.07
27	85	Dry	1	294.2	294.2	—	16.12
28	85	Dry	2	294.2	490.3	—	28.89
29	85	Dry	0.5	490.3	326.9	—	21.74
30	85	Dry	1	490.3	490.3	—	25.50
31	50	Dry	0.5	98.1	65.4	—	3.22
32	50	Dry	1	98.1	98.1	—	5.58
33	50	Dry	2	98.1	163.4	—	9.26
34	50	Dry	1	196.1	196.1	—	8.77
35	50	Dry	2	196.1	326.9	—	14.66
36	50	Dry	0.5	294.2	196.2	—	9.03
37	50	Dry	1	294.2	294.2	—	11.34
38	50	Dry	2	294.2	490.3	—	18.61
39	50	Dry	0.5	490.3	326.9	—	15.07
40	50	Dry	1	490.3	490.3	—	18.62

back-pressure and the desired confining stress were then applied. The status of saturation was monitored through the six piezometers installed in the specimen. In the six saturated chamber specimens shown in Table 3, the average B parameter from the piezometer readings after 2 h of saturation ranged from 0.95 to 0.98. Considering the compressibility of MLS, these B values should correspond to a degree of saturation in excess of 99.8% according to Black and Lee (1973).

Variables applied in the calibration tests include initial D_r of the specimen, effective vertical stress σ_v', and the ratio of effective horizontal stress σ_h'/σ_v' (K). Table 3 summarizes these applied variables. All tests used stress-controlled vertical and horizontal boundary conditions. Dynamic compaction was an important part of the construction activities in Mai-Liao. The upper K values shown in Table 3 were selected to reflect a moderately to highly overconsolidated stress history due to dynamic compaction.

CPT chamber test results

There were a total of 40 chamber CPT performed in this series of experiments, as shown in Table 3. Six of them were performed in a saturated specimen using a standard (35.6 mm diameter) piezocone to evaluate the development of excess pore pressure during cone penetration. The porous element was located immediately behind the cone tip. The remaining CPT were conducted in a dry specimen using a half-size (17.8 mm diameter) cone. Figure 14 depicts the q_c, friction ratio FR, and excess pore pressure Δu obtained from Test 4. The corresponding piezometer readings obtained dur-

Fig. 14. CPT results of Test 4.

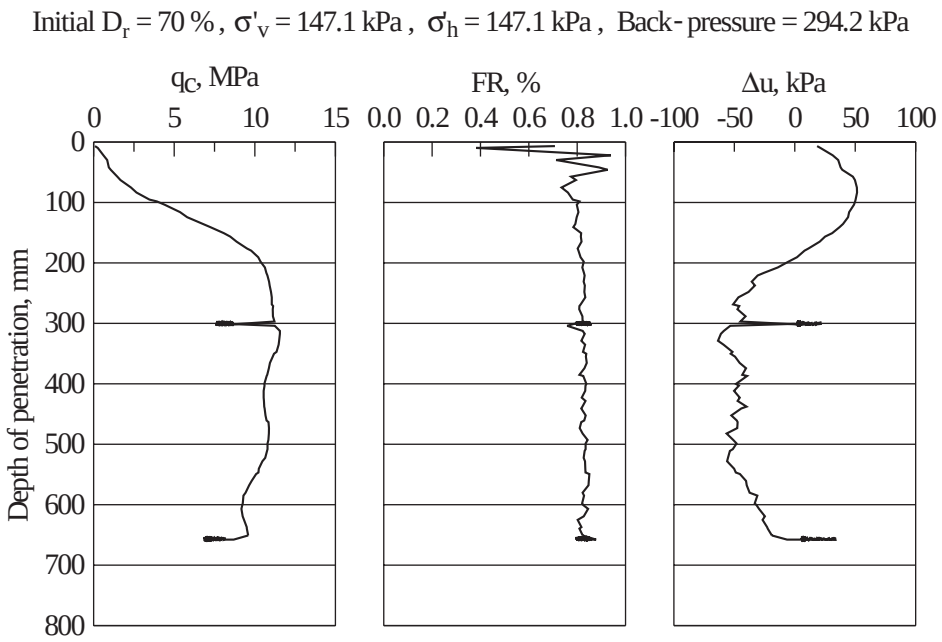

Fig. 15. Excess pore pressure measurements from piezometers in Test 4.

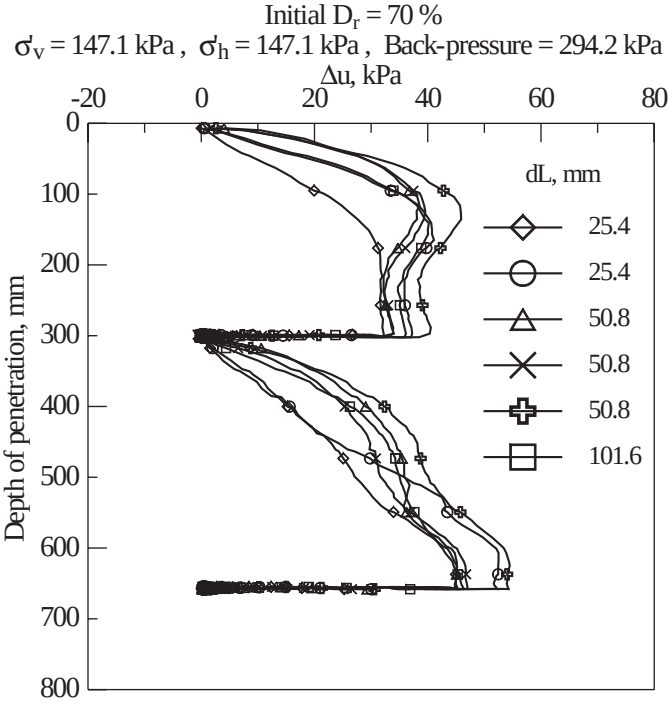

ing cone penetration are shown in Fig. 15. CPT is known for its capability of sensing thin layers of soils with different properties. The relatively smooth q_c profiles are an indication of reasonable uniformity of the specimens. The excess pore pressure obtained in the piezometers during Test 4 had a maximum value of approximately 50 kPa. The excess pore pressure measurement on the cone was negative, after a stable q_c was reached (i.e., beyond a depth of 200 mm). There is no apparent relationship between the excess pore pressure and distance between the pizometer and center of the specimen, as shown in Fig. 15. In Test 4, the cone penetration was interrupted at 300 mm and the excess pore pressure was allowed to dissipate before further penetration. The full dissipation of excess pore pressure took approximately 25 s. According to McNeilan and Bugno (1984), the q_c values immediately after restart of the penetration can be at least 20% higher than that just prior to the interruption for CPT in silt or sandy silt. The discrepancy in q_c is a result of high pore pressure development during cone penetration in silt. For the test shown in Fig. 14, the peak q_c after restart was 11.55 MPa, which is 4% higher than the q_c recorded just prior to the interruption of penetration, and much lower than those reported by McNeilan and Bugno (1984).

The major differences between Tests 6 and 7 (see Table 3) are the cone diameter and saturation of the chamber specimen. The diameter ratio for the half-size cone used in Test 7 is 30, which is twice that of Test 6. If the effect of excess pore pressure development or change of diameter ratio is significant, the q_c of the half-size cone (i.e., Test 7) in a dry specimen should be significantly larger than that of the standard cone (i.e., Test 6) in a saturated specimen. Figure 16 shows the q_c profiles from these two tests. The average q_c taken at depths between 200 and 500 mm, where they have reached a plateau, agree within 4%. Observation in Tests 4, 6, and 7 indicate that CPT in MLS is essentially a drained test. The following analysis of CPT data makes no distinction between CPT in dry and saturated specimens. Also, because the excess pore pressure development was minimal, no pore pressure correction was made to convert q_c to q_T.

The insensitivity of q_c to the change in diameter ratio, comparable with CPT calibration tests in very loose uniform quartz sand (Parkin 1988), is a direct reflection of the compressible (or lack of dilatancy) nature of MLS. An important additional implication is that the chamber specimen is large enough even for a standard cone penetrometer and there should be insignificant boundary effects. The use of a half-size cone is an additional assurance of minimal boundary effects.

Fig. 16. Comparison of q_c profiles from tests with two different cone diameters.

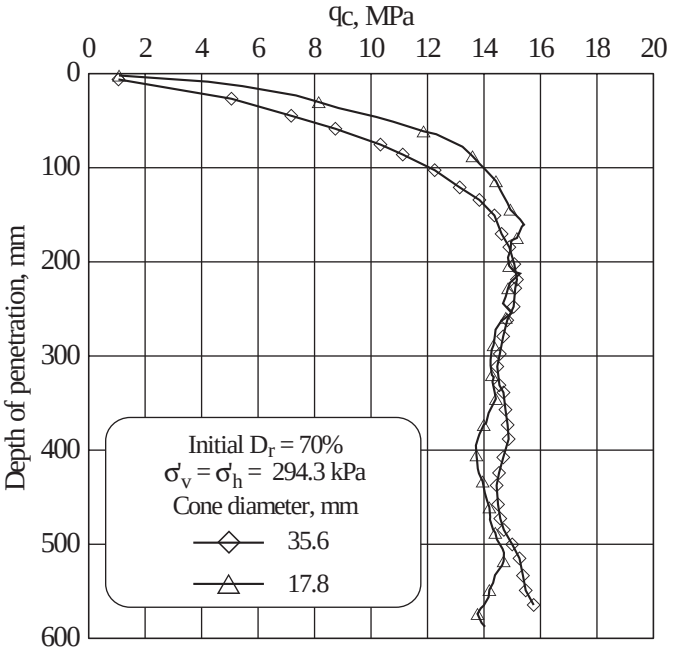

Figure 17 shows the averaged q_c values and their relationship with initial σ_h' in the specimen. The average q_c is determined based on readings taken in calibration tests at depths from 200 to 500 mm where q_c has reached more or less a steady value. The q_c in MLS has a clear and positive relationship with σ_h'. The influence of σ_h' appears to be much stronger than the initial D_r. The relationship between q_c and σ_v' is not nearly as obvious as shown in Fig. 18. For low-compressibility sand, there have been conflicting reports on the relationship between q_c and σ_h' (Houlsby and Hitchman 1988; Huang and Ma 1994). In practice at least, σ_h' in sand is rarely determined based on q_c, as the noise of q_c may be more significant than the effects of σ_h'. The trend shown in Fig. 17 is an indication that for a high-compressibility sand such as MLS, there is the potential to determine σ_h' using q_c.

Comparisons with CPT in clean, uniformly graded quartz sand

Because of the high compressibility of MLS, the change of void ratio or D_r after the specimen is subjected to a confining stress is significant. Monitoring the change of void ratio was difficult for the chamber specimens, especially when they were dry. Four sets of compression tests on saturated specimens in a triaxial cell were performed to determine the void ratio under a variety of initial states. The four K values shown in Table 3 were used in each of the four sets of compression tests. The confining stress was increased in steps following a given K value. The same initial D_r and stress conditions used in chamber tests were duplicated in these compression tests. The same specimen preparation, saturation, and testing procedures as described previously for isotropic compression tests were followed. The results of the compression tests are plotted in Fig. 12 in terms of void ratio versus effective mean normal stress and referred to as the CPT initial states. These initial states, which consider the effects of sand compression due to consolidation, are used in the following analysis for the CPT data in MLS.

Fig. 17. q_c versus σ_h'.

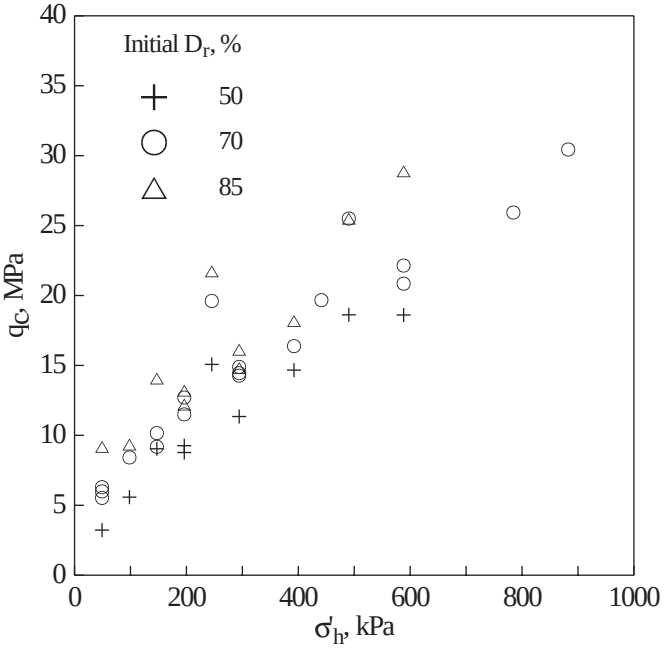

Fig. 18. q_c versus σ_v'.

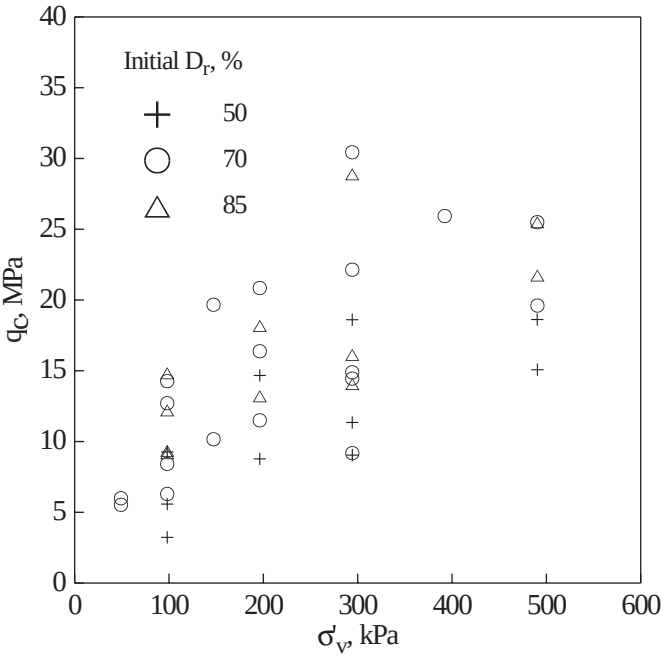

Grain crushing of MLS occurs even under mild stress conditions, as demonstrated in Fig. 12. The framework proposed by Konrad (1998) provides a system where the effects of grain crushing are integrated in the interpretation of CPT in sand. The interpretation is based on normalized q_c, normalized state parameter ($\psi_N = \psi/(e_{max} - e_{min})$), initial state stress (p'_0), and the stress at critical state (p'_{cs}). The main purpose of normalization is to minimize the effects from differences in p'_0, range of void ratios (i.e., $e_{max} - e_{min}$), and p'_{cs} for vari-

Fig. 19. Normalized q_c versus ψ_N.

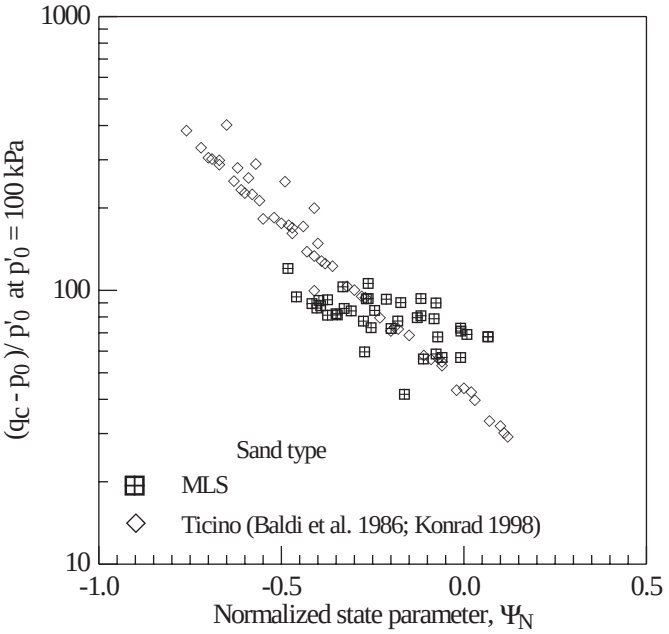

ous soil types. Using Ticino sand and a p'_0 of 100 kPa as a reference, it is possible to obtain a unique normalized q_c for several types of sand, as reported by Konrad (1998). This framework offers an ideal platform where q_c in MLS can be compared with a clean, uniformly graded sand, such as Ticino sand, considering the differences in dilatancy, gradation, and grain crushing characteristics.

Figure 19 compiles MLS chamber CPT data along with Ticino sand reported by Baldi et al. (1986) and Konrad (1998). The q_c value is normalized following an empirical equation by Konrad (1998) for a reference p'_0 of 100 kPa as

$$[4] \qquad \left(\frac{q_c - p_0}{p'_0}\right)_{p'_0=100\text{kPa}} = \frac{q_c - p_0}{p'_0}\left(\frac{p'_0}{100}\right)^{0.373}$$

where p_0 is the total mean stress at initial state. For the range of ψ_N and p'_0 applied, the data points of MLS are clustered within a rather narrow range of normalized q_c. This is an indication that for a given initial stress state, q_c in MLS is considerably less sensitive to ψ_N (or relative density) in comparison with Ticino sand. The phenomenon is consistent with the result depicted in Fig. 17 where initial σ_h' shows a much stronger influence than D_r.

The framework by Konrad (1998) calls for a further normalization to consider the differences in p'_{cs} that relate to grain crushing. In this case, the normalized q_c obtained in eq. [4] is multiplied by the ratio of ($p'_{csTicino}$ / p'_{csMLS}) that corresponds to the same ψ_N. The last normalization should bring MLS data points closer to those of the Ticino sand, according to Konrad (1998). However, due to the drastic differences in λ_c between MLS and Ticino sand, as shown in Fig. 12, ($p'_{csTicino}$ / p'_{csMLS}) increases significantly with ψ_N. As a result, the p'_{cs} normalization would shift MLS data points into a trend that is opposite to that of the Ticino sand (i.e., normalized q_c increases with ψ_N), which is apparently unrealistic. The p'_{cs} normalization implicitly assumes that for a given p'_0 and ψ_N, sand of different types near the cone tip during penetration should have similar dilative or contractive behavior. Or, the state paths should follow the same direction to reach critical state where grain crushing occurs under high-stress conditions. This assumption would be valid for most of the clean, uniformly graded quartz sand with comparable compressibility. As reported in Fig. 8, the compressibility of MLS can be many times higher, especially under high stresses. It is thus expected that MLS near a penetrating cone tip is much more contractive than Ticino sand under the same p'_0 and ψ_N. For Konrad's (1998) framework to be valid, it is necessary to account for such differences in sand compressibility. For MLS, it may require the choice of p'_{cs} that corresponds to a lower ψ_N than that in Ticino sand. The current framework, however, does not provide a basis for an appropriate selection of that ψ_N.

Fig. 20. Comparison between measured q_c and q_c computed using eq. [5].

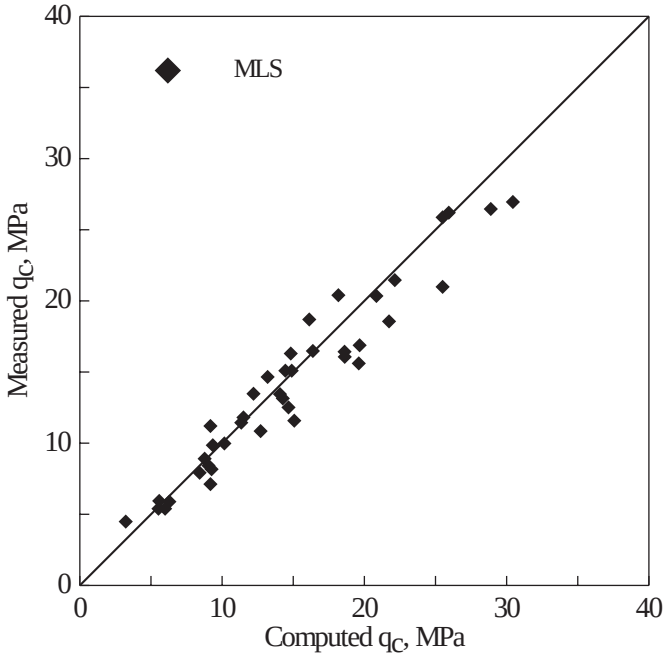

The above analysis provides convincing evidence that a separate method is called for when interpreting CPT in MLS. The CPT calibration data in MLS were compiled and an empirical equation that relates q_c to D_r and state of stress was developed. This equation follows the pattern of Fioravante et al. (1991) that considers the effects of σ_v' and σ_h' as follows:

$$[5] \qquad q_c = 230(\sigma_v')^{0.108}(\sigma_h')^{0.425}\exp(1.45D_r)$$

Note that D_r used in eq. [5] is calculated based on void ratios after the application of confining stress. Figure 20 shows a comparison between q_c values obtained in the available chamber CPT and those estimated using eq. [5]. The coefficient of correlation is 0.966.

Concluding remarks

The paper compiled and analyzed a series of in situ test data on MLS, a relatively compressible silty fine sand. Laboratory experiments were performed to determine the compressibility, shear strength, and dilatancy of MLS that has a

fines content of approximately 15%. A series of CPT were conducted in a calibration chamber to evaluate the possible differences between tests in MLS and those in clean, uniformly graded quartz sand. Based on the findings of these studies, the following conclusions are made.

(1) For a compressible sand such as MLS, the change in void ratio as a result of static loading can be many times that of a clean, uniformly graded quartz sand. The effects of compressibility should not be ignored for MLS in the interpretation of test data.

(2) The ϕ'_{crit} of MLS is comparable with the lower end of a quartz sand. However, the range of $\phi'_{max} - \phi'_{crit}$ for MLS is relatively small compared with quartz sand. This is a result of the lack of dilatancy of MLS.

(3) For a given initial stress state, q_c in MLS is considerably less sensitive to ψ_N (or relative density) in comparison with clean quartz sand.

(4) Normalizing CPT results in MLS following the framework proposed by Konrad (1998), without considering that the differences of compressibility may be unrealistic. The analysis of available data provides convincing evidence that a separate method is called for when interpreting CPT in MLS.

(5) For MLS, there appears to be a consistent relationship between q_c and σ_h'. The q_c values obtained from available chamber CPT show a coefficient of correlation of 0.966 with those estimated using the empirical equation developed herein.

(6) The laboratory experiments described in this paper are restricted to MLS with a fines content of approximately 15%. Further studies are necessary to determine the effects of different fines contents on the behavior of MLS.

Acknowledgments

This research was conducted under a contract with the Construction Engineering Division of the Formosa Plastics Group, Taipei, Taiwan. The National Science Council of the Republic of China provided additional funding under contracts 82-0115-E-009-373 and 83-0410-E-009-026.

References

Baldi, G., Belloti, R., Ghiona, V., Jamiolkowski, M., and Pasqualini, E. 1986. Interpretation of CPTs and CPTUs. Part 2. Drained penetration of sands. *In* Proceedings of the Fourth International Geotechnical Seminar on Field Instrumentation and in situ Measurements, Nanyang Technological Institute, Singapore, pp. 129–156.

Been, K., and Jefferies, M.G. 1985. A state parameter for sands. Géotechnique, **35**(2): 99–112.

Been, K., Jefferies, M.G., and Hachey, J. 1991. The critical state of sands. Géotechnique, **41**(3): 365–381.

Bellotti, R., and Pedroni, S. 1991. Design and development of a small calibration chamber for compressible sands. *In* Proceedings of the First International Symposium on Calibration Chamber Testing, Potsdam, N.Y. *Edited by* A.-B. Huang. Elsevier, New York, pp. 91–100.

Bishop, A.W., and Green, G.E. 1965. The influence of end restraint on the compression strength of a cohesionless soil. Géotechnique, **15**(3): 243–266.

Black, D.K., and Lee, K.L. 1973. Saturating laboratory samples by back pressure. Journal of the Soil Mechanics and Foundation Engineering Division, ASCE, **99**(1): 75–93.

Bolton, M.D. 1986. Strength and dilatancy of sands. Géotechnique, **36**(1): 65–78.

El-Sohby, M.A., and Andrawes, K.Z. 1972. Deformation characteristics of granular materials under hydrostatic compression. Canadian Geotechnical Journal, **9**(3): 338–350.

Fioravante, V., Jamiolkowski, M., Tanizawa, F., and Tatsuoka, F. 1991. Result of CPTs in Toyoura quartz sand. *In* Proceedings of the First International Symposium on Calibration Chamber Testing, Potsdam, N.Y. *Edited by* A.-B. Huang. Elsevier, New York, pp. 135–146.

Hardin, B.O. 1985. Crushing of soil particles. Journal of the Geotechnical Engineering Division, ASCE, **111**(10): 1177–1192.

Houlsby, G.T., and Hitchman, R. 1988. Calibration chamber tests of a cone penetrometer in sands. Géotechnique, **38**(1): 39–44.

Huang, A.B., and Ma, M.Y. 1994. An analytical study of cone penetration tests in granular material. Canadian Geotechnical Journal, **31**(1): 91–103.

Huang, A.B., Bunting, R.D., and Carney, T.C. 1991. Piezoblade tests in a clay chamber. *In* Proceedings of the First International Symposium on Calibration Chamber Testing, Potsdam, N.Y. *Edited by* A.-B. Huang. Elsevier, New York, pp. 161–174.

Ishihara, K. 1993. Liquefaction and flow failure during earthquakes. The 33rd Rankine Lecture. Géotechnique, **43**(3): 351–415.

Joustra, K., and de Gijt, J.F. 1982. Results and interpretation of cone penetration tests in soils of different mineralogical composition. *In* Proceedings of the Second European Symposium on Penetration Testing, Amsterdam, The Netherlands, Vol. 2, pp. 615–626.

Koerner, R.M. 1970*a*. Effect of particle characteristics on soil strength. Journal of the Soil Mechanics and Foundation Engineering Division, ASCE, **96**(4): 1221–1234.

Koerner, R.M. 1970*b*. Behavior of single mineral soils in triaxial shear. Journal of the Soil Mechanics and Foundation Engineering Division, ASCE, **96**(4): 1373–1390.

Konrad, J.M. 1998. Sand state from cone penetrometer tests: a framework considering grain crushing stress. Géotechnique, **48**(2): 201–215.

Kulhawy, F.H., and Mayne, P.W. 1991. Relative density, SPT, and CPT interrelationships. *In* Proceedings of the First International Symposium on Calibration Chamber Testing, Potsdam, N.Y. *Edited by* A.-B. Huang. Elsevier, New York, pp. 197–211.

Lade, P.V., Yamamuro, J.A., and Bopp, P.A. 1996. Significance of particle crushing in granular materials. Journal of the Geotechnical Engineering Division, ASCE, **122**(4): 309–316.

Lee, K.L., and Farhoomand, I. 1967. Compressibility and crushing of granular soils in anisotropic triaxial compression. Canadian Geotechnical Journal, **4**(1): 68–86.

McNeilan, T.W., and Bugno, W.T. 1984. Cone penetration test results in offshore california silts. *In* Proceedings of the Symposium on Strength Testing of Marine Sediments: Laboratory and in-situ Measurements, San Diego, Calif. ASTM STP 883, pp. 55–71.

Mesri, G., Feng, T.W., and Benak, J.M. 1990. Postdensification penetration resistance of clean sands. Journal of the Geotechnical Engineering Division, ASCE, **116**(7): 1095–1115.

Parkin, A.K. 1988. The calibration of cone penetrometers. *In* Proceedings of the First International Symposium on Penetration Testing, ISOPT-1, Orlando, Fla. *Edited by* De Ruiter. Balkema, Rotterdam, The Netherlands, pp. 221–243.

Rix, G.J., and Stokoe, K.H. 1991. Correlation of initial tangent modulus and cone penetration resistance. *In* Proceedings of the First International Symposium on Calibration Chamber Testing,

Potsdam, N.Y. *Edited by* A.-B. Huang. Elsevier, New York, pp. 351–362.

Salgado, R., Mitchell, J.K., and Jamiolkowski, M. 1997. Cavity expansion and penetration resistance in sand. Journal of Geotechnical and Geoenvironmental Engineering, ASCE, **123**(4): 344–354.

Vesic, A.S., and Clough, G.W. 1968. Behavior of granular materials under high stresses. Journal of the Soil Mechanics and Foundation Engineering Division, ASCE, **94**(3): 661–688.

Voyiadjis, G.Z., Kurup, P.U., and Tumay, M.T. 1993. Preparation of large-size cohesive specimens for calibration chamber testing. Geotechnical Testing Journal, ASTM, **16**(3): 339–349.

Yamamuro, J.A., Bopp, P.A., and Lade, P.V. 1996. One dimensional compression of sands at high pressures. Journal of the Geotechnical Engineering Division, ASCE, **122**(2): 147–154.

Yu, H.S., and Houlsby, G.T. 1991. Finite cavity expansion in dilatant soils: loading analysis. Géotechnique, **41**(1): 173–183.